Switchable Fresnel lens based on micropatterned alignment

Xiao-Qian Wang, Abhishek K. Srivastava,* Vladimir G. Chigrinov, and Hoi-Sing Kwok

*Department of Electronic and Computer Engineering, Hong Kong University of Science and Technology,
Clear Water Bay, Kowloon, Hong Kong, China*
Corresponding author: abhishek_srivastava_lu@yahoo.co.in

In this Letter we disclose a method to fabricate a liquid crystal (LC) Fresnel zone lens (FZL) with higher efficiency. The LCFZL, based on alternate twisted nematic (TN) and planar aligned (PA) regions, has been prepared by means of a two-step photo-alignment process. The FZL profile for both optical regimes, i.e., in TN and PA alignment domains, generates the same focal length (f). Thus, the proposed LCFZL manifests double light intensity at the focal point and therefore offers double the efficiency of existing FZLs. Moreover, because of lower driving voltage and fast response, these elements could find application in many modern devices. © 2013 Optical Society of America

OCIS codes: (220.0220) Optical design and fabrication; (230.0230) Optical devices; (250.6715) Switching.
http://dx.doi.org/10.1364/OL.38.001775

The fast switchable Fresnel zone lens (FZL) with high efficiency is in high demand for a variety of applications and therefore has attracted many researchers in recent years [1–6]. There are two very common approaches for fabricating a liquid crystal (LC) FZL. The first approach employs patterned electrodes to generate a periodic electrical field distribution to control locally the LC director [1]. The second approach deals with initially guided LC directors to realize a periodic refractive index distribution (e.g., patterned polymer relief [7,8], polymer dispersed LCs [9,10], polymer-stabilized LCs [11–13], dye doped LCs [14–17], and UV-modified alignment films [4,5]).

Recently, Lu *et al.* have proposed a 2D/3D switchable display based on a switchable LCFZL by employing patterned electrodes [1]. The proposed structure improves the optical quality; however, the switching time of their LCFZL is ~0.35 s. In another approach, modification of the LC alignment by means of UV exposure was used to fabricate the LCFZL [5]. This fabrication process is complicated and requires high exposure energies to generate the LCFZL profile. Moreover, the switching OFF time (~180 ms) is very large.

Lou *et al.* have proposed using nano-imprinting to ease fabrication of the LCFZL [8]. A metal shim made of nickel was used as master stamp to create the FZL profile on a UV-curable prepolymer film. Although this approach is simpler, it is hampered by both issues with the master stamp and the response time of the LCFZL.

All of the device approaches described above are characterized by low efficiency, complicated fabrication procedure, and long switching time (hundreds of millisecond). In contrast, the photoalignment process affords easy fabrication of the LCFZL with higher efficiency.

In this Letter, we disclose a method to fabricate an LCFZL device based on patterned photoalignment layers. The photopatterned LCFZL shows a total switching response time (OFF + ON) of 6.7 ms at a drive voltage < 4 V/μm (peak-to-peak) of an arbitrary wave. This photopatterned LCFZL makes use of alternatively distributed twisted nematic (TN) and planar aligned (PA) alignment domains. Figure 1 shows a schematic representation of the photopatterned LCFZL in the cross sectional view.

The white region represents the TN domain while the black region corresponds to PA domain. Additionally, the LCFZL design shown in Fig. 1 requires one optically active alignment layer in order to tune its focal length f optically. The optical tunability is discussed later in the Letter.

The photoaligned LCFZL cell shown in Fig. 1 employs two substrates with different alignment layers. One layer (polyimide, PI-3744, Chisso Co. Japan) is optically passive and provides a fixed alignment direction. The second layer [SD1, a sulfonic azo dye provided by Dai-Nippon Ink and Chemicals (DIC), Japan] is optically active and its orientation direction can be changed by exposing it again with polarized light. When the SD1 layer is exposed using polarized light ($\lambda = 450$ nm), the energy absorbed by SD1 molecules is proportional to the $\cos^2 \theta$, where the angle θ characterizes the orientation of dye molecules with respect to the polarization vector of the exposing light [18]. In other words, the probability distribution is nonuniform and has an angular dependence. Therefore, the populations of azo-dye molecules that have their transition dipole moments parallel to the direction of the plane of polarization of the pumping light receive excess energy. As a result, these dye molecules reorient from their initial orientation. This process produces an excess of chromophores in a direction where the absorption oscillator of SD1 is perpendicular to the plane of the polarization of the pumping light [18]. Exposing the
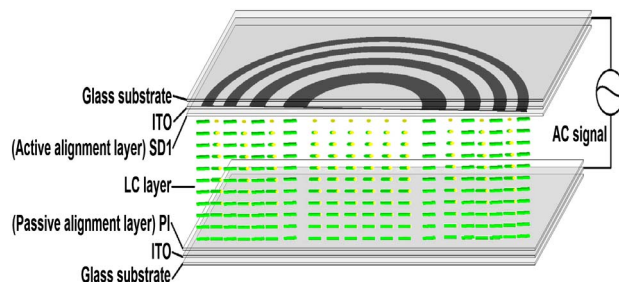

Fig. 1. Configuration of the designed LCFZL. One ITO coated glass substrate has its inner surface coated with a PI layer, while the other substrate is coated with an SD1 layer. White and black regions represent the TN and PA domains, respectively.

SD1 layer with 450 nm polarized light results in alignment in the direction perpendicular to the plane of polarization of the pumping light with high anchoring energy and almost zero pre-tilt angle.

The LCFZL cell was fabricated from two indium tin oxide (ITO) coated glass substrate (thickness = 0.5 mm). One substrate was coated with PI-3744 and rubbed unidirectionally, while the other substrate was coated with SD1 (1 wt. % in N,N-dimethylformamide). The two coated substrates were assembled to form an LC cell with a 3 μm thick cell gap. The cell was initially exposed with linearly polarized light ($\lambda = 450 \pm 10$ nm light divergence $< 1°$) at an exposure dose of 5 J/cm^2. The same cell was turned $90°$ and exposed again (with the same exposure dose) through a FZL photo mask that was in close contact with the cell and was designed to meet the condition $R_k^2 = k\lambda f,\ k = 1, 2, 3....$ The SD1 molecules in the exposed areas were realigned with their easy axis orthogonal to the original orientation, and the fabricated cell shows the FZL profile. An LC material (LC A-0138 from DIC) was injected into the cell by capillary action. This LC material has a $\Delta n \approx 0.18$ and shows a first Mauguin minimum for 632.8 nm light for the designed 3 μm-thick cell [18].

In the absence of an electric field, the light passes through the LCFZL cell and results in redistribution of energy for the outward beam and thus generates the FZL pattern. When an electric field of arbitrary waveform is applied, all LC molecules in both alignment domains switch to the vertical position and the FZL pattern disappears. Figures 2(a) and 2(b) show an optical photomicrograph of the LCFZL (lens I) with a focal length f of 3.2 mm under parallel polarizers with the easy axis of the PA domain (white region) parallel to the polarizer. The black region represents the TN domain. Figure 2(c) shows an optical photomicrograph of the LCFZL (lens II) with $f = 50$ mm under crossed polarizers, where the white and black regions represents TN and PA alignment domains, respectively.

A He–Ne laser ($\lambda = 632.8$ nm) was used to study different features of the photoaligned LCFZL. The laser beam size was expanded by a factor of 10 using a beam expander and the LCFZL pattern was projected onto a screen at a distance of ~250 cm from the LCFZL device. Several images of the FZL pattern were captured using a digital SLR camera (Canon EOS 600D), and the captured images were analyzed using MATLAB.

The optical axis of the polarizer was set to be parallel to the PI rubbing direction of the LCFZL cell. Because the two output beams from the two different alignment regions do not interfere with each other [19], the proposed

LCFZL is more efficient, as the two Fresnel zone plates are merged into one.

The on-axis wave amplitude at primary focus for the zone lens with an even and odd number of zones has been expressed in [20], which suggests that the constructive focal point for both the odd and even zones of the photoaligned LCFZL is at the same position. As a result, the light intensity for both the odd and even zones, which is proportional to E^2, adds up and consequently increases the diffraction efficiency by two times as compared to previously reported LCFZL devices.

Figure 3 shows the diffraction profile of the photoaligned LCFZL. Figures 3(a) and 3(b) represent the diffractive state of lens I ($f = 3.2$ mm) and lens II ($f = 50$ mm), respectively. Figure 3(c) shows the nondiffractive state for lens I, which is exactly the same for lens II. In Figs. 3(d) and 3(e), the profiles of the light intensity distribution for Figs. 3(a) and 3(b) are shown, respectively. When an electric field of $U \gg$ threshold voltage is applied, both the PA and TN region represent the same optical state where the LC molecules are vertically aligned. At this electric field magnitude, the diffraction pattern disappears.

In the theoretical calculation, the electric field of the incident light is E_{in}, with its linear polarization parallel to the x axis (easy axis of PI layer), given by $E_{\text{in}} = \begin{bmatrix} E_0 \\ 0 \end{bmatrix}$. The outgoing field E_{out} through the odd and even zones of the LC zone lens can be defined as $E_{\text{out/odd}} = \begin{bmatrix} 0 \\ E_0 \end{bmatrix}$ & $E_{\text{out/even}} = \begin{bmatrix} E_0 e^{\text{in}\frac{2\pi d}{e}/\lambda} \\ 0 \end{bmatrix}$, respectively, where n_e is the refractive index of the LC, λ is the incident wavelength, and d is the thickness of the LC cell. The first-order diffracted light field D_1 is given by

$$D_1 = \frac{\int_0^{2A_1} E_{\text{out|odd}} e^{-i2\pi(A/2A_1)} \mathrm{d}A}{2A_1} + \frac{\int_0^{2A_1} E_{\text{out|even}} e^{-i2\pi(A/2A_1)} \mathrm{d}A}{2A_1}$$

$$= \frac{E_0}{2\pi} \begin{bmatrix} 2i e^{\text{in}_e \frac{2\pi}{\lambda} d} \\ -2i \end{bmatrix}, \tag{1}$$

(a)   **(b)**   **(c)**

(d)   **(e)**

Fig. 3.   Diffraction pattern for the designed LCFZL. (a) Diffractive state of lens I, (b) diffractive state of lens II, (c) dark or nondiffractive state of lens I at the electric field of 10 V, (d) the light intensity profile for lens I, and (e) the light intensity profile for lens II.
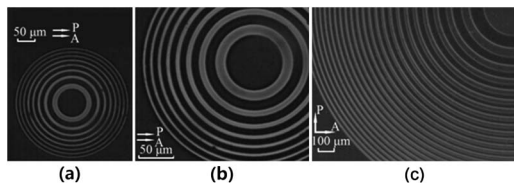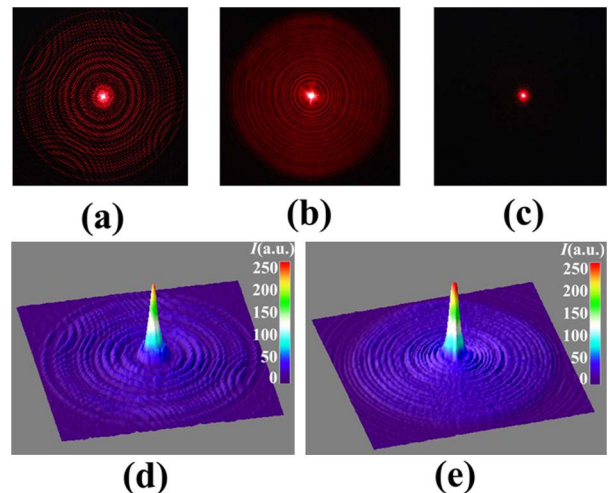

Fig. 2.   Optical microphotograph of the designed LCFZL. (a) LCFZL (lens I) with $f = 3.2$ mm under parallel polarizers, (b) the enlarged image of the lens I shown in (a), and (c) LCFZL (lens II) with $f = 50$ mm under crossed polarizers.

where A_1 is the area of the first odd zone. Therefore, the theoretical diffraction efficiency for the first-order diffracted beam is given by $\eta_1 = (|D_1|^2/|E_{in}|^2) = (2/\pi^2)$ [21].

In our experiments, the light intensity I_1 of the first-order diffracted light was measured at the primary focal point by subtracting the zeroth-order light intensity in the center of the diffraction pattern. The diffraction efficiency is given by $\eta = I_1/I_0$ (where I_0 is the incident light intensity), and the value measured ($\sim$19.1%) is close to the theoretical limit [21]. The small LC declination at the boundary of the TN and PA alignment domains can account for the slightly lower observed efficiency than expected from theoretical predications.

The device response time, expressed as the ON-time (τ_{on}) and OFF-time (τ_{off}), respectively, for the photoaligned LCFZL is governed by the TN domains and thus is exactly the same as the response times for a TN cell. The measured response time values are $\tau_{on} \approx 100$ µs and $\tau_{off} \approx 6.6$ ms, with the total switching time $\sim$6.7 ms. This total switching time is faster than existing devices [18,22] and can be improved further by optimizing the LC and cell parameters [18,19].

An additional advantage of the photoaligned LCFZL is that the FZL pattern can be erased and rewritten with different f by using a polarized laser ($\lambda = 450 \pm 10$ nm) [22]. The speed of pattern erasing and rewriting is the same and depends on the anchoring energy of the alignment layer and elastic parameters of the LC [23]. The anchoring energy of the optically active alignment layer can be tuned by using controlled doses of the exposing laser energy. With a high power laser as the optical write/erase source and proper selection of LC parameters, an optical response time of <100 ms is achievable [23].

In summary, we have demonstrated a switchable LCFZL with a diffraction efficiency of $\sim$19%, and response time of $\sim$6.7 ms. As compared to existing devices, the photoaligned LCFZL shows faster response and consumes less power. The use of a photoalignment layer on one substrate in conjunction with a fixed alignment layer on a second substrate makes the fabrication process simpler and cheaper than for previously reported devices. The active photoalignment layer also allows tuning of the focal length f of the LCFZL cell by exposing it through a FZL mask of different f using a polarized 450 nm laser. Minimizing the divergence of the laser and maintaining very close contact of the FZL mask with the cell are both critically important in achieving high resolution. The response time for optical tunability of f depends on the LC parameters and the incident power of the laser, and could be <100 ms. With these features of fast switching, low power consumption, and tunability

of f, these photoaligned LCFZL elements could find applications in many modern optical and electro-optical devices.

References

1. J. G. Lu, X. F. Sun, Y. Song, and H. P. D. Shieh, J. Disp. Technol. **7**, 215 (2011).
2. C. Dorrer, S. K. H. Wei, P. Leung, M. Vargas, K. Wegman, J. Boulé, Z. Zhao, K. L. Marshall, and S. H. Chen, Opt. Lett. **36**, 4035 (2011).
3. X. Q. Wang, F. Fan, J. T. Sun, L. Wang, A. Srivastava, and V. G. Chigrinov, Mol. Cryst. Liq. Cryst. **559**, 228 (2012).
4. S. J. Hwang, T. A. Chen, K. R. Lin, and S. C. Jeng, Appl. Phys. B **107**, 151 (2012).
5. S. C. Jeng, S. J. Hwang, J. S. Horng, and K. R. Lin, Opt. Express **18**, 26325 (2010).
6. M. S. Millán, E. Pérez-Cabré, and J. Otón, J. Phys. Condens. Matter **139**, 012016 (2008).
7. C. R. Lee, K. C. Lo, and T. S. Mo, Jpn. J. Appl. Phys. **46**, 4144 (2007).
8. Y. M. Lou, Q. K. Liu, H. Wang, Y. C. Shi, and S. L. He, Appl. Opt. **49**, 4995 (2010).
9. H. Jashnsaz, N. H. Nataj, E. Mohajerani, and A. Khabbazi, Appl. Opt. **50**, 4295 (2011).
10. H. Ren, Y. H. Fan, and S. T. Wu, Appl. Phys. Lett. **83**, 1515 (2003).
11. Y. H. Fan, H. Ren, and S. T. Wu, Opt. Express **11**, 3080 (2003).
12. H. Nemati, E. Mohajerani, A. Moheghi, M. B. Rad, and N. H. Nataj, Europhys. Lett. **87**, 64001 (2009).
13. Y. H. Fan, H. Ren, and S. T. Wu, Opt. Express **13**, 4141 (2005).
14. L. C. Lin, H. C. Jau, T. H. Lin, and A. Y. Fuh, Opt. Express **15**, 2900 (2007).
15. L. C. Lin, K. T. Cheng, C. K. Liu, C. L. Ting, H. C. Jau, T. H. Lin, and A. Y. G. Fuh, Proc. SPIE **6911**, 69110I (2008).
16. K. T. Cheng, C. K. Liu, C. L. Ting, and A. Y. G. Fuh, Opt. Express **15**, 14078 (2007).
17. Y. Li, Y. S. Yu, L. Guo, S. Z. Wu, C. Chen, L. G. Niu, A. W. Li, and H. Yang, J. Opt. **12**, 035203 (2010).
18. V. Chigrinov, V. Kozenkov, and H. S. Kwok, *Photoalignment of Liquid Crystalline Materials: Physics and Applications.* (Wiley, 2008).
19. L. Vicari, *Optical Applications of Liquid Crystals.* (IOP Publishing, 2003).
20. A. S. Marathay and J. F. McCalmont, J. Opt. Soc. Am. A **21**, 510 (2004).
21. K. C. Lo, J. D. Wang, and C. R. Lee, Appl. Phys. Lett. **91**, 181104 (2007).
22. F. Fan, A. K. Srivastava, V. G. Chigrinov, and H. S. Kwok, Appl. Phys. Lett. **100**, 111105 (2012).
23. J. T. Sun and V. G. Chigrinov, Mol. Cryst. Liq. Cryst. **561**, 1 (2012).